Journal of Power Sources 273 (2015) 608–612

Contents lists available at ScienceDirect

Journal of Power Sources

journal homepage: www.elsevier.com/locate/jpowsour

Short communication

Application of a bio-derivative, rosin, as a binder additive for lithium titanium oxide electrodes in lithium-ion batteries

So-Jin Kim, Bo-Ram Lee, Eun-Suok Oh*

School of Chemical Engineering, University of Ulsan, 93 Daehakro, Nam-gu, Ulsan 680-749, Republic of Korea

HIGHLIGHTS

- Bio-derived rosin is used for the first time as a binder additive for LTO electrodes.
- The addition of rosin decreases the crystallinity of PVdF binder.
- Rosin aids in the dispersion and the lithium-ion diffusion of the LTO electrodes.
- The addition of 40 wt% rosin to PVdF significantly improves the LTO performance.

GRAPHICAL ABSTRACT

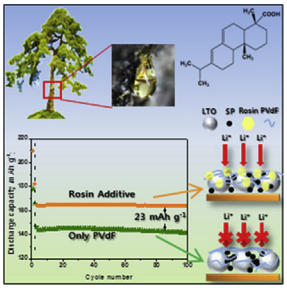

ARTICLE INFO

Article history:
Received 19 July 2014
Received in revised form
20 September 2014
Accepted 25 September 2014
Available online 2 October 2014

Keywords:
Rosin
Polyvinylidene fluoride
Binder
Lithium titanium oxide
Lithium-ion battery

ABSTRACT

Rosin, which is an extract of pine trees, is used as an eco-friendly binder additive to a conventional solvent-based binder, polyvinylidene fluoride (PVdF). The composite binder system is used to evaluate the performance of the $Li_4Ti_5O_{12}$ (LTO) electrodes using a range of physical and electrochemical characterization techniques. The addition of rosin decreases the crystallinity of PVdF, disperses the conducting agent and binder well, and ultimately leads to an increase in the diffusivity and cyclic capacity of lithium ions. When the amount of rosin additive to the PVdF binder is 40 wt%, the LTO electrode exhibits the highest cyclic capacity and diffusivity; of 164 mAh g^{-1} at the 110th cycle and 4.28 × 10^{-10} cm^2 s^{-1}, respectively.

1. Introduction

Rechargeable batteries have been adopted widely in a variety of applications ranging from portable devices to electric vehicles. To enhance the battery performance, the components of the electrodes, such as the active materials, need to be improved. Among the components of the electrodes, considerable attention has recently been paid to the binder because it is a critical factor for the cyclic performance, particularly of high-capacity active materials [1–4]. The polymeric binder provides integrity among the active materials, conductive additive, and current collector to form an electrical network in the electrode. Polyvinylidene fluoride (PVdF) is the most widely used binder in LIBs because of its excellent electrochemical stability, good wettability with the electrolyte and acceptable adhesion capability. On the other hand, PVdF is a semi-crystalline polymer so that lithium ion transport through the crystalline phase to the active materials is suppressed because parts of the active materials are covered with the PVdF binder [4–6]. In addition, weak interactions between the active materials and PVdF binder lead to the discrete aggregate distribution of PVdF on the surface of the active materials, resulting in the coarse dispersion of electrodes [6].

* Corresponding author. Tel.: +82 52 259 2783; fax: +82 52 259 1689.
E-mail address: esoh1@ulsan.ac.kr (E.-S. Oh).

http://dx.doi.org/10.1016/j.jpowsour.2014.09.160
0378-7753/

Together with PVdF, water-based styrene-butadiene rubber (SBR) has been also applied to commercial LIBs in combination with a carboxy-methyl cellulose (CMC) thickening agent [7]. In addition, a range of polymers including bio-derivative polymers have been studied to enhance the electrochemical performance of LIBs by substituting conventional PVdF and SBR/CMC [1–4,8,9]. Furthermore, there have been a few studies on the binder other than changing the types of polymers. Conducting fillers, such as graphene [10] and acetylene black [11] were used to increase the electrical conductivity of the insulating polymer binder, and consequently improve the electrode performance. A conducting adhesive layer, which is composed of conducting polymer composites, between the electrode and current collector enhanced the cyclic performance of LIB significantly by improving the adhesion [12]. On the other hand, there have been few studies on the additives for changing the characteristics of the polymer binder, e.g., increasing the dispersion of the binder.

In this study, a bio-derivative, rosin, which is a type of acidic resin obtained from pine or conifer trees, was introduced as an additive for a conventional PVdF binder of $Li_4Ti_5O_{12}$ (LTO) electrodes. LTO is an attractive candidate for anode materials because its volume is nearly unchanged during the charging and discharging process and high operating voltage at 1.55 V (vs. Li/Li^+), leading to a long cycle life and high rate capability [13]. A variety of physical and electrochemical characterization techniques have been adopted to examine the roles of rosin additives in the LTO electrodes.

2. Experimental

Commercially available PVdF (Solef 5130, Solvay Plastics) and rosin (Alfa Aesar) were used as a polymer binder and additive in LTO (Posco ESM Co., $d_{avg} = 10$ μm) electrodes. PVdF contains a certain amount of functional groups in its polymer chain to improve the interactions with active materials. Initially, some rosin was fully dissolved in *N*-methyl-2-pyrrolidine (NMP) and PVdF powders were then added to the solution. The mixture was stirred at high temperatures (>70 °C) for 24 h to dissolve and fully mix the PVdF with rosin. The weight ratios between PVdF and rosin in the binder solution were 100:0, 95:5, 80:20, 60:40, and 50:50, respectively, which are noted as PVdF, PVdFr5, PVdFr20, PVdFr40, and PVdFr50.

To manufacture the electrode slurry, 85 wt% LTO was mixed with a 10 wt% binder solution and 5 wt% super-P in a zirconia jar using a planetary ball mill (Pulverisette 7, Fritsch; speed 380 rpm) for 1 h. The resulting slurry was coated on copper-foil (20 μm) and dried in a convection oven at 130 °C for 20 min followed by vacuum drying at 80 °C for 24 h. CR2016 coin-half cells were assembled in an argon-filled glove box using lithium metal as the counter electrode and 1 M $LiPF_6$ (Panaxetec Co., Korea) dissolved in a 1:1:1 (v/v/v) mixture of ethylene carbonate/ethylmethyl carbonate/dimethyl carbonate as the electrolyte.

The interactions between PVdF and rosin in the fabricated binder were analyzed by Fourier transform infrared spectroscopy (FT-IR, Thermo Scientific, Nicolet IR 200). Differential scanning calorimetry (DSC, Q20, TA Instruments) of the binder films were performed under a nitrogen atmosphere between 30 and 220 °C at a 10 °C heating/cooling rate. The morphology of the electrodes was examined by field emission scanning electron microscopy (FE-SEM, Carl Zeiss, Supra40) with an energy dispersive spectrometer (EDS, Oxford Ltd.). The coin cells are charged and discharged galvanostatically within a voltage range of 1–2.6 V in a battery cycler (PNE solution Co., Korea). Cyclic voltammetry (CV) and electrochemical impedance spectroscopy (EIS) were conducted using a spectroscopy (VSP, BioLogic Science Instruments) at various scan rates from 0.5 to 20 mV s^{-1} between 1 and 2.6 V, and at a frequency range of 100 kHz to 0.01 Hz, respectively.

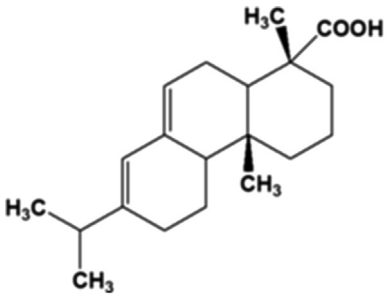

Fig. 1. Chemical structure of abietic acid, the main component of rosin.

3. Results and discussions

Rosin is a hard and yellowish solid produced by distilling the sticky liquid resin of pine or conifer trees, and is composed of mainly abietic acid, as illustrated in Fig. 1. The material is generally used as an additive for paper sizing, soap, sealing wax, and adhesives owing to its excellent water resistance, low softening point, and high acid value. The change in the degree of crystallinity of PVdF due to the addition of such rosin additives was examined by DSC, and the results are shown in Table 1 (see also Supporting Information Fig. S1). The degree of crystallinity was calculated from the ratio of the melting enthalpy of the samples to that of 100% crystalline PVdF polymer (104.5 J g^{-1}) [14]. The crystallinity of the PVdF decreased with increasing rosin content, though the reason for the slight increase in the crystallinity of PVdFr5 is unclear. The melting temperature that is associated with the lamellae thickness of PVdF [15] also decreased with increasing rosin content. This suggests that the rosin additive in PVdF causes partial deconstruction of the crystallites with a change in its lamellae thickness.

Such a structural change was also expected from the FT-IR results in Fig. 2, suggesting a change in the interaction of carboxyl groups. As mentioned earlier, the PVdF used in this study contained a certain number of functional groups, which were inferred to be carboxylic acids due to O–H and C=O stretching vibrations at 1722, 1760, and 3529 cm^{-1} [16]. The coexistence of the monomeric (peaks at 1760 and 3529 cm^{-1}) and dimeric carboxyl acids (peak at 1722 cm^{-1}) suggests that some of the carboxyl groups in PVdF form hydrogen bonds with each other. Pure rosin forms primarily hydrogen-bonded dimers, which are illustrated by the strong and broad O–H stretching absorption between 2500 and 3300 cm^{-1}, including the peaks at 2539 and 2650 cm^{-1}, and the C=O stretching band of the dimer near 1722 cm^{-1}. When the rosin content in PVdF was increased, the peaks at 1760 and 3529 cm^{-1}, which were assigned to the C=O and O–H stretching band in the monomeric state, decreased gradually and disappeared. This means that rosin forms a new interaction with the carboxyl groups of PVdF through hydrogen bonds, which is responsible for the change in PVdF crystalline structure observed by DSC analysis. As mentioned previously, the change in the crystallinity of PVdF binder can affect

Table 1
Melting temperature and enthalpy of the PVdF samples containing the rosin additive measured by DSC.

Sample	T_m, °C	ΔH_m, J g^{-1}	Crystallinity, %
PVdF	163.07	31.93	30.56
PVdFr5	161.96	33.84	32.38
PVdFr20	162.47	21.03	20.12
PVdFr40	160.59	16.68	15.96
PVdFr50	159.18	13.40	12.82

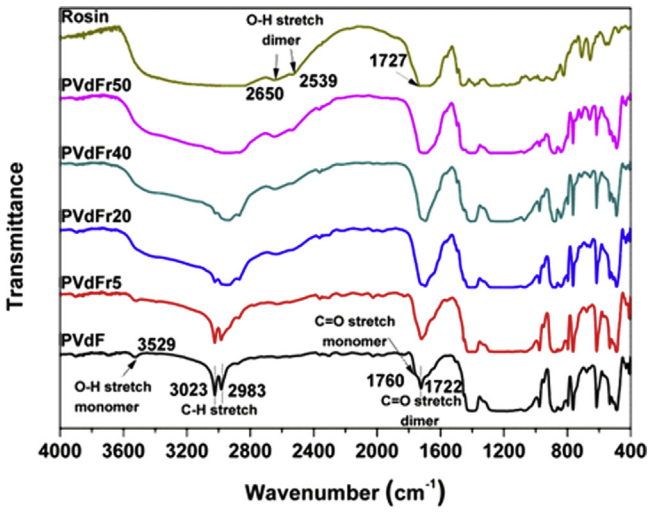

Fig. 2. FT-IR spectra of PVdF, PVdFr5, PVdFr20, PVdFr40, PVdFr50 and pure rosin samples.

lithium ion transport in LIB electrodes. Thus, a LTO anode is chosen to clearly see the effect of the rosin additive because it is more appropriate to a high-rated electrode, which requires rapid lithium ion transport, than a common graphite electrode.

To examine the effects of the change in binder crystallinity on the dispersion of LTO electrodes, SEM with EDS mapping of the LTO electrodes containing 10 wt% PVdF/rosin binders was performed, and the results are displayed in Fig. 3. The SEM images in Fig. 3(a–e) show an improvement in the homogeneous morphology of the LTO electrodes with increasing amount of rosin in PVdF. In addition, the EDS mapping images of Fig. 3(f–j) confirm an even dispersion of carbon atoms, representing super-P as a conductive agent and binder, through the addition of rosin. The polymeric binder was reported to be a critical factor for the homogeneity of electrodes [17–19]. Li et al. [19] showed that an ionic polymer, ammonium polyacrylic acid, improved the dispersion of $LiCoO_2$ cathodes by an electrostatic and steric stabilization mechanism. Similarly, the carboxyl groups in rosin are ionized in the binder solution and form a repulsive force field to alleviate the agglomeration of LTO and super-P particles while the electrode slurry is dried. Moreover, the decrease in the crystallinity of PVdF makes the polymer more flexible during the drying process, which may also contribute to a better dispersion when rosin is used as an additive of the PVdF binder. The Brunauer–Emmett–Teller (BET) surface area confirmed the better dispersion of the rosin-added PVdF binder. The BET surface area of the LTO electrodes was increased with the addition of rosin; 2.15 $m^2\ g^{-1}$ for the PVdF, 5.61 $m^2\ g^{-1}$ for the PVdFr20, and 8.83 $m^2\ g^{-1}$ for the PVdFr40 electrodes, respectively.

In addition, the X-ray photoelectron spectra of the LTO electrodes in Fig. 4 were quite interesting. As the rosin content increased, the C 1s peak at 289.7 eV (Fig. 4a) corresponding to carbon in PVdF decreased gradually on the surface of the electrodes, whereas the intensity of the Ti 2p peaks in Fig. 4b increased because the absolute amount of PVdF in the LTO electrode decreases so that a broader surface of titanium is exposed directly to the electrolyte. Without discussing the oxidation state of Ti atoms, a positive shift in the Ti 2p doublet occurs as the rosin content is increased. Normally, the positive shift is caused by an increase in the oxidation state of titanium from Ti^{3+} to Ti^{4+} [20]. Alternatively, Zhao et al. [21] presented a positive shift in the binding energy corresponding to Ti 2p of LTO when smaller LTO particles were well dispersed in the electrode. Although this is consistent with the present results, a further detailed study may clarify the positive shift by the addition of rosin.

Cyclic tests with rate performance of the LTO electrodes were performed within a potential range of 1–2.6 V (vs. Li^+/Li) with various current densities between 0.1 and 20 C, and their results are shown in Fig. 5a. When rosin was used as an additive to binder, the initial discharge capacity of the LTO electrodes increased from 178 mAh g^{-1} to 209 mAh g^{-1}. Here the capacities were calculated on the basis of the weight of active materials, LTO. The increase in capacity was attributed to the contribution of carboxyl group by providing sites for lithium adsorption [22]. Unfortunately, the functional groups lead simultaneously to an increase in the irreversible capacity by trapping the adsorbed lithium ions. The addition of rosin also increases the cyclic capacity of the LTO electrode, particularly 164 mAh g^{-1} at the 110th cycle of 1 C for the LTO/PVdFr40 electrode, whereas the LTO/PVdF system shows 141 mAh g^{-1}. Consistent with previous studies [17,19], the homogeneous distribution in the composite electrode by the addition of rosin allows even utilization of LTO particles, resulting in an increase in cyclic capacity. The increase in the oxidation state of titanium inferred from the XPS results in Fig. 4 might contribute to the increased cyclic capacity. On the other hand, the addition of more than 50 wt% rosin weakened the adhesion strength of PVdF seriously, which might be responsible for the reduction of the capacity when the PVdFr50 was used as the binder. From the high rate tests exhibited in Fig. 5a, it is clear that regardless of the use of the

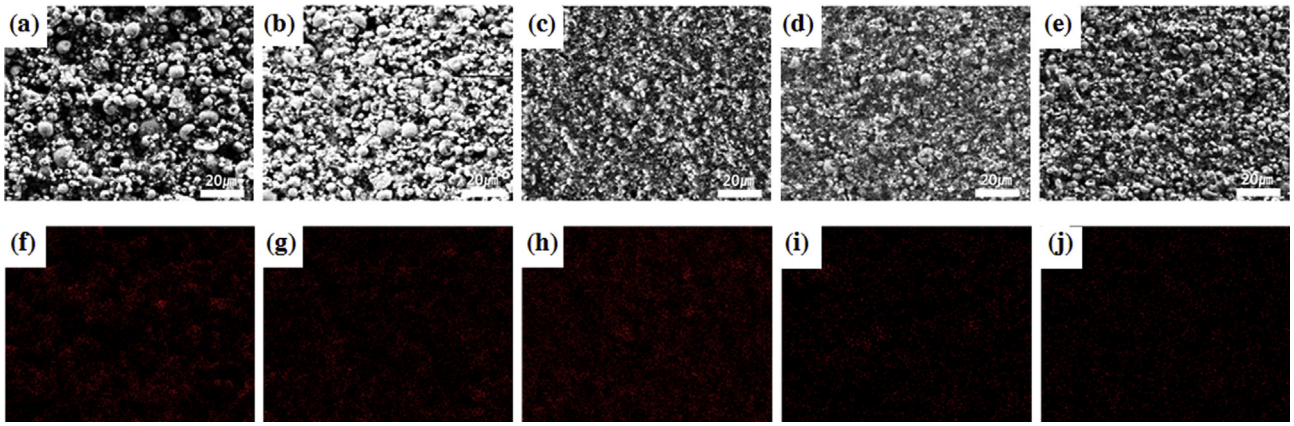

Fig. 3. SEM images of the LTO electrodes using (a) PVdF, (b) PVdFr5, (c) PVdFr20, (d) PVdFr40 and (e) PVdFr50 binders (f–j) EDS mapping profiles of carbon on (a–e) SEM images, respectively.

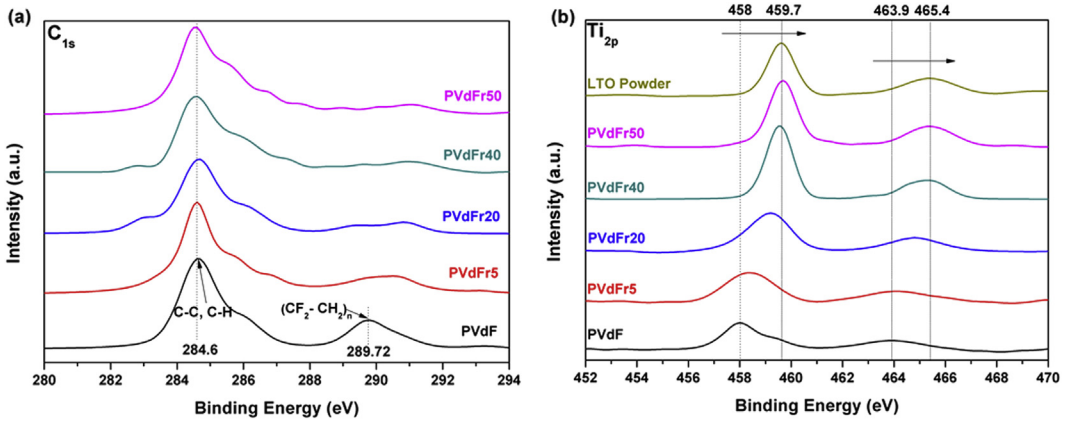

Fig. 4. XP spectra of (a) C 1s and (b) Ti 2p of the LTO electrodes containing PVdFr binders.

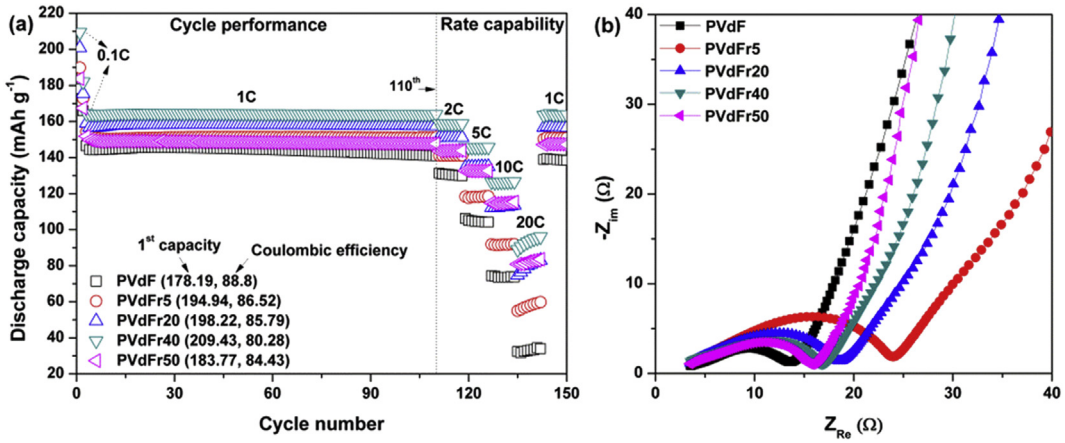

Fig. 5. (a) Cycle performances and rate capabilities at various C-rates and (b) EIS results of the LTO electrodes.

rosin additive, the samples fully restore their capacities after high rate charge/discharge cycles up to 20 C. The EIS result in Fig. 5b can support the cell performance in Fig. 5a. The decrease in the amount of crystalline PVdF binder in the composite electrode gives rise to more LTO surface exposed directly to the electrolyte along with rapid lithium ion transport, leading to a decrease in charge transfer resistance, which is represented by the size of the semicircles in the medium frequency region of Fig. 5b. Additionally, using the low-frequency Warburg region of the EIS, the diffusion coefficients of lithium ions (D_{Li}) can be calculated from.

$$D_{Li} = \frac{R^2T^2}{2A^2n^4F^4C_{Li}^2\sigma^2}, \quad (1)$$

where R, T, A, n, F, and C_{Li} are gas constant, temperature, surface area, number of electron transfer, Faraday constant, and concentration of lithium ions in solid, respectively [23,24]. The value of σ indicates the slope of real or imaginary part of impedance versus $\omega^{-0.5}$ (frequency in the Warburg region). The diffusion coefficients calculated using Eq. (1) were 2.06×10^{-10} for PVdF, 3.44×10^{-10} for PVdFr5, 3.15×10^{-10} for PVdFr20, 4.28×10^{-10} for PVdFr40 and 3.14×10^{-10} cm^2 s^{-1} for the PVdFr50 electrodes, respectively.

To examine lithium ion transport in detail, CV of the samples was performed with a variety of scan rates between 0.5 and 20 mV s^{-1}. Fig. 6 shows the representative CV results at 0.5 and 20 mV s^{-1} (inset). Except for the LTO electrode containing low adhesive PVdFr50 binder, the redox peaks become intense and close as the rosin content increases, demonstrating better electrode kinetics with the rosin additive. This may be attributed to the increase in the oxidation state of titanium and well dispersion of LTO, confirmed by the peak shifts of XPS in Fig. 4. Compared to the other electrodes, therefore, the LTO electrode containing PVdFr40 binder

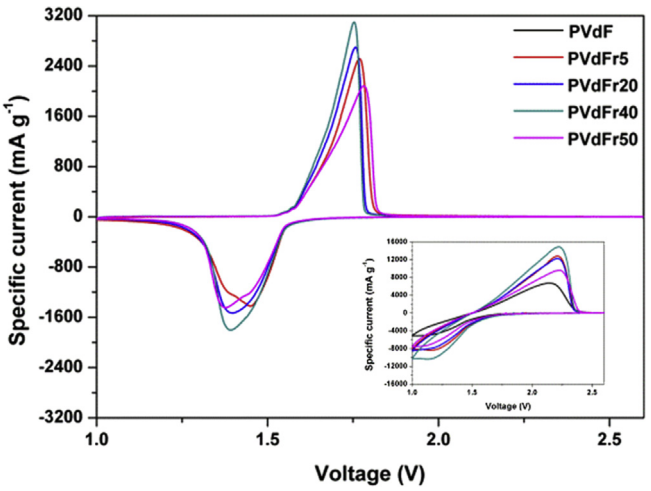

Fig. 6. CV of the LTO electrodes at 0.5 mV s^{-1} (inset 20 mV s^{-1}).

exhibited sharper redox peaks with high current and smaller gap between the redox peaks, suggesting that the PVdFr40 binder has relatively low resistance for the redox mechanism. A linear fit can be drawn from these CV profiles (see Supporting Information Fig. S2). According to the Randles–Sevcik equation [25],

$$i_p = 2.69 \times 10^5 n^{3/2} C_{Li} A D_{Li}^{1/2} \nu^{1/2}, \quad (2)$$

the diffusion coefficients of lithium ions can be also calculated from the slope between the peak current, i_p, and the square root of the scan rate, v. Similar to the results calculated from the EIS, the PVdF40 and PVdF electrodes have the highest and lowest diffusion coefficients (see Supporting Information Fig. S2), even though the magnitudes are quite a bit different because the Randles–Sevcik Eq. (2) is appropriate to solution-based diffusion, not solid-based diffusion. Therefore, the decrease in the crystallinity of the binder and the good dispersion in the electrode, particularly the LTO electrode containing 40 wt% rosin additive, ultimately improves the cell performance of the LTO electrodes.

4. Conclusions

A bio-derivative, rosin, is used for the first time as an additive to a conventional PVdF binder. The rosin additive newly forms an interaction with the functional groups in the binder, leading to the partial deconstruction of the PVdF crystallites with a change in the lamellae thickness. In addition, the repulsive force formed by the carboxyl groups of rosin helps disperse the components of the electrodes, resulting in an increase in the cyclic capacity including initial capacity with increasing rosin content. The improvement in lithium ion diffusion and charge transfer by the addition of rosin is also responsible for the better rate capability of the LTO electrode compared to the LTO/pure PVdF electrode. On the other hand, a rosin content greater than 50 wt% undermines the adhesion and has an adverse effect on the electrochemical performance of the LTO electrodes. This beneficial effect of the rosin additive can be applied to other binders or electrode systems to enhance the LIB performance.

Acknowledgments

The work was supported by the Ministry of Science, ICT and Future Planning (NRF-2009-C1AAA001-2009-0093307). Support was also provided by the Basic Science Research Program through the National Research Foundation of Korea (NRF) funded by the Ministry of Education, Science and Technology (2010-0024077).

Appendix A. Supplementary data

Supplementary data related to this article can be found at http://dx.doi.org/10.1016/j.jpowsour.2014.09.160.

References

[1] I. Kovalenko, B. Zdyrko, A. Magasinski, B. Hertzberg, Z. Milicev, R. Burtovyy, I. Luzinov, G. Yushin, Science 334 (2011) 75–79.
[2] S. Komaba, K. Shimomura, N. Yabuuchi, T. Ozeki, H. Yui, K. Konno, J. Phys. Chem. C. 115 (2011) 13487–13495.
[3] G. Liu, S. Xun, N. Vukmirovic, X. Song, P. Olalde-Velasco, H. Zheng, V.S. Battaglia, L. Wang, W. Yang, Adv. Mater. 23 (2011) 4679–4683.
[4] H.-K. Park, B.-S. Kong, E.-S. Oh, Electrochem. Commun. 13 (2011) 1051–1053.
[5] Z. Zhong, Q. Cao, B. Jing, X. Wang, X. Li, H. Deng, Mater. Sci. Eng. B 177 (2012) 86–91.
[6] M. Yoo, C.W. Frank, S. Mori, Chem. Mater. 15 (2003) 850–861.
[7] H.S. Kim, K.Y. Chung, B.W. Cho, J. Power Sources 189 (2009) 108–113.
[8] M. Murase, N. Yabuuchi, Z.J. Han, J.Y. Son, Y.T. Cui, H. Oji, S. Komaba, ChemSusChem 5 (2012) 2307–2311.
[9] L. Gong, M.H.T. Nguyen, E.-S. Oh, Electrochem. Commun. 29 (2013) 45–47.
[10] S.W. Han, S.J. Kim, E.-S. Oh, J. Electrochem. Soc. 161 (2014) A587–A592.
[11] G. Liu, H. Zheng, S. Kim, Y. Deng, A.M. Minor, X. Song, V.S. Battaglia, J. Electrochem. Soc. 155 (2008) A887–A892.
[12] S. Lee, E.-S. Oh, J. Power Sources 244 (2013) 721–725.
[13] Y.J. Hao, Q.Y. Lai, D.Q. Liu, Z.U. Xu, X.Y. Ji, Mater. Chem. Phys. 94 (2005) 382–387.
[14] G. Teyssedre, A. Bernes, C. Lacabanne, J. Polym. Sci. Part B: Polym. Phys. 31 (1993) 2027–2034.
[15] K. Nakagawa, Y.J. Ishida, J. Polym. Sci. Part B: Polym. Phys. Ed. 11 (1973) 2153–2171.
[16] Infrared Spectrometry. https://www2.chemistry.msu.edu/faculty/reusch/virttxtjml/spectrpy/infrared/irspec1.htm. (accessed July 5, 2014).
[17] B. Lestriez, C. R. Chim. 13 (2010) 1341–1350.
[18] G. Liu, H. Zheng, X. Song, V.S. Battaglia, J. Electrochem. Soc. 159 (2012) A214–A221.
[19] C.-C. Li, J.-T. Lee, X.-W. Peng, J. Electrochem. Soc. 153 (2006) A809–A815.
[20] T. Hanawa, J. Periodontal Implant Sci. 41 (2011) 263–272.
[21] Y. Zhao, G. Liu, L. Liu, Z. Jiang, J. Solid State Electrochem 13 (2009) 705–711.
[22] A. Magasinski, B. Zdyrko, I. Kovalenko, B. Hertzberg, R. Burtovyy, C.F. Huebner, T.F. Fuller, I. Luzinov, G. Yushin, ACS Appl. Mater. Interfaces 2 (2010) 3004–3010.
[23] N. Takami, A. Satoh, M. Hara, T. Ohsaki, J. Electrochem. Soc. 142 (1995) 371–378.
[24] C. Lin, X. Fan, Y. Xin, F. Cheng, M.O. Lai, H. Zhou, L. Lu, J. Mater. Chem. A 2 (2014) 9982–9993.
[25] J.R. Dahn, J. Jiang, L.M. Moshurchak, M.D. Fleischauer, C. Buhrmester, L.J. Krausec, J. Electrochem. Soc. 152 (2005) A1283–A1289.